Analyzing Importance Measure Methodologies for Integrated Probabilistic Risk Assessment in Nuclear Power Plants

Tatsuya Sakurahara[a*], Seyed Reihani[a], Mehmet Ertem[a], Zahra Mohaghegh[a], and Ernie Kee[b]

[a] Department of Nuclear, Plasma, and Radiological Engineering, University of Illinois at Urbana-Champaign, IL, USA

[b] YK.Risk, LLC, TX, USA

Abstract: Importance Measures (IMs) are used to rank the risk contributing factors in Probabilistic Risk Assessment (PRA). In this paper, existing IM methodologies are analyzed in order to select the most suitable IM for an *Integrated* PRA (IPRA) of Nuclear Power Plants. In IPRA, the classical PRA of the plant is used, but specific areas of concern (e.g., fire, GSI-191, organizational factors, and seismic) are modeled in a simulation-based module (separate from PRA) and the module is then linked to the classical PRA of the plant. The IPRA, with respect to modeling techniques, bridges the classical PRA and simulation-based/dynamic PRA. This paper compares the local and Global Importance Measure (GIM) methodologies and explains the importance of GIM for IPRA. It also demonstrates the application of GIM methodologies to illustrative examples and, after comparing the results, selects the CDF-based sensitivity indicator ($S_i^{(CDF)}$) as an appropriate moment-independent GIM for IPRA. The results demonstrate that, because of the complexity and nonlinearity of IPRA frameworks, $S_i^{(CDF)}$ is the best method to accurately rank the risk contributors. $S_i^{(CDF)}$ can capture three key features: (1) distribution of input parameters, (2) interactions among input parameters, and (3) distribution of the model output.

Keywords: Importance Measure, Integrated Probabilistic Risk Assessment (IPRA), Global Importance Measure, Global Sensitivity Analysis, Simulation-based PRA

1. BACKGROUND

Classical IMs are developed to provide insight into the relative ranking of risk contributing factors (e.g., components, input parameters) in PRA [1]. This paper focuses on the comparative studies of IM methods and the selection of an IM approach for an *Integrated* Probabilistic Risk Assessment (IPRA) framework. Our ultimate goal in using an IM method is to find the most critical factors of NPP risk and rank the factors based on the degree of their contribution to the system risk (i.e., Core Damage Frequency). This would guide us to dedicate more resources and time to assess the accuracy and validity of the values (and associated uncertainties) of the most critical factors in the risk models and, ultimately, reduce the system risk.

Several of the authors of this paper proposed an IPRA framework for diverse applications such as: (1) incorporation of the effects of organizational factors into PRA [2,3], (2) risk-informed resolution of Generic Safety Issue 191 (GSI-191) [4], (3) advancement of fire PRA analysis [5,6], and (4) improvement of seismic PRA [7]. The IPRA, with respect to modeling techniques, bridges classical and simulation-based/dynamic PRA. The static nature of classical PRA was the main impetus for having created a dynamic PRA. Although a simulation-based/dynamic PRA is the ideal goal for nuclear power risk analysis, it is, on a short-term basis, impractical and quite costly. Currently, NPPs utilize classical PRAs and to change them to fully simulation-based PRAs would require significant time and resources. In the IPRA framework, the classical PRA of the plant would be used, but specific areas of concern (e.g., organizational factors, fire, GSI-191, and seismic) would be modeled in a simulation-based module (separate from PRA) and the module would then be linked to the classical plant-specific PRA model.

Figure 1: Schematic representation of Integrated Probabilistic Risk Assessment (IPRA).

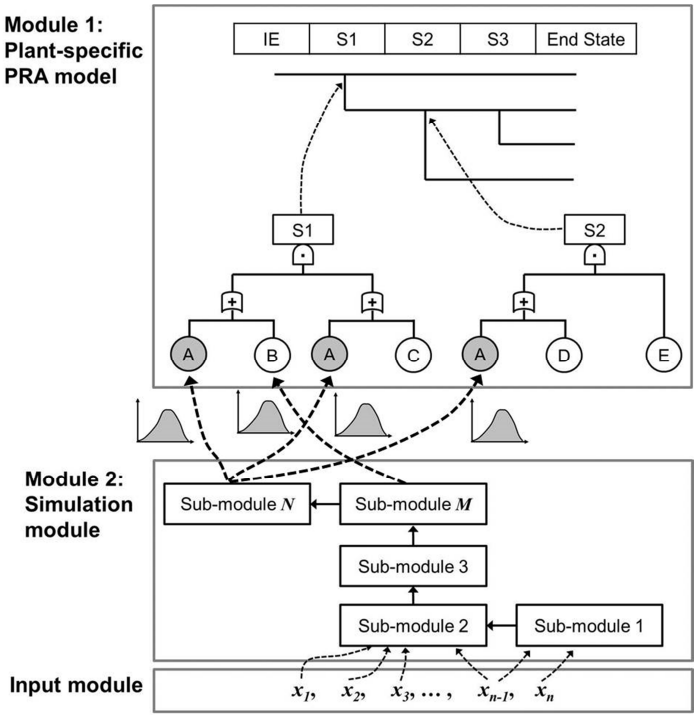

The major features of an IPRA framework (Figure 1) are: (1) Classical plant-specific PRA and a (2) Simulation module that includes simulation and uncertainty quantification of realistic physical or social phenomena affecting certain basic events of plant-specific PRA. An IPRA approach would provide the possibility of (a) advancing quantification of dynamic interactions, (b) depicting a more adequate representation of contextual factors (e.g., physical factors and human performance), and (c) advancing propagation of uncertainties in the physical or social phenomena leading to specific basic events in PRA. These three improvements would lead to more "realistic" modeling of underlying failure mechanisms of specific basic events of classical PRA. Such modeling improvements, when used in IPRA applications, could be used to help improve safety and efficiency in NPP design and operation. Another advantage of IPRA is that it is a step toward having a fully simulation-based PRA. If and when NPPs are ready to switch to simulation-based PRAs, the simulation modules of an IPRA approach would be appropriate engines for them.

The IM methodology has not yet been applied to IPRA. This is due to the intrinsic difficulties in applying the traditional IM methodologies such as Fussell-Vesely (FV) Importance Measure and Risk Achievement Worth (RAW) [1] to IPRA. Since the conventional IM methodologies are designed for ranking the basic events, their application to IPRA which includes explicit variables (e.g., physical parameters such as temperature and pressure), in Module 2 of Figure 1, is not well defined. Moreover, there is a concern over the potential bias caused by traditional IM methodology when it is applied to IPRA. The input variables of IPRA are given in various units and wide ranges, unlike basic event probabilities in classical PRA that are dimensionless and defined between 0 and 1. Thus, the traditional IM methodology, which evaluates the importance of risk factors based on the change of risk metrics, can result in the biased ranking of risk factors. Another deficiency of conventional IM methodologies is that they evaluate the ranking of risk factors (e.g., input parameters, failure probability of basic events) "locally", i.e., based on the derivative of risk metrics with respect to one risk factor in the proximity of its nominal value. More detailed discussion on local and global importance measure methodologies follows in Section 2.

Section 2.1 compares the local and Global IM (GIM) methodologies and explains the need for GIM for IPRA. Section 2.2 demonstrates GIMs and selects one, the CDF-based sensitivity indicator ($S_i^{(CDF)}$) [8], as an appropriate IM methodology for IPRA. In Section 3, the one-way Sensitivity Analysis (SA) method and $S_i^{(CDF)}$ are applied to two example models to compare the results of these two different methodologies. In addition, based on a comparison of these methodologies, the appropriateness of $S_i^{(CDF)}$ for IPRA is discussed. Finally, the conclusion and the future plans for this research are presented in Section 4.

2. SELECTION OF IMPORTANCE MEASURE METHODOLOGY FOR IPRA

2.1. Local vs. Global Importance Measures

Importance measures (IMs) are commonly used to rank structures, systems and components with respect to their risk significance. Several IM methods have been developed for this purpose. These methods can be categorized into two groups; local IMs and Global IMs (GIMs). The local IMs are basically defined by an approximation to the partial derivative of the model output with respect to a specific input parameter in the proximity of its nominal value [9]. Examples of local IMs include Fussell-Vesely (FV) [1], Risk Achievement Worth (RAW) [1] and Differential Importance Measure (DIM) [8]. These IMs evaluate the influence of the deviation of an input parameter on the model output (usually risk metrics in PRA) when one input parameter is perturbed from its nominal value, while the other input parameters remain fixed at their nominal values.

In reality, risk metrics are formulated as a function of input parameters, and these input parameters are mostly uncertain and expressed by probability distributions. Local IMs cannot reflect the entire distribution of input parameters, because their scope is inherently limited to the output variation around the nominal output, calculated by fixing all but one input parameter to their nominal values [10]. Moreover, local IMs are not capable of taking into account the non-linearity of the risk model or the interaction among input parameters [11]. This is because the concept of a partial derivative of a model output, with respect to one of the input parameters around its nominal value, can be valid as an IM only if the risk model is linear and there are no significant interactions among input parameters.

As it appears in existing literature, Global Sensitivity Analysis (GSA) has been extensively studied in order to discover the sensitivity level of input parameters on the output measure. GSA also helps uncover the model errors, rank the importance of input parameters according to their effect on the output measure specifically to simplify the complex models, and identify the critical regions of the input vector space [12]. Another important aspect of GSA is the consideration of the interaction of input parameters on the result of the output measure. Designs of experiments, metamodels, and regression analysis techniques have been developed for this purpose [12]. For instance, R.J. Tebbens et al. [13] performed SA on their model of post-eradication polio risk using the regression analysis technique. In their work, the regression model was developed by randomly sampling the input parameters from their continuous distribution. Then, the sensitivity of each input parameter was evaluated based on Spearman's rank correlation, which indicates the extent of monotonic relationships between model output and input parameters.

Recently, GIM methods have been proposed to account for the entire distribution of the input parameters and the model output in risk models in order to evaluate the effect of an input parameter with respect to the model uncertainty [14]. The GIMs evaluate the change of model output when all input parameters are randomly sampled from their distribution [10]. Thus, they are able to take into account the entire distribution of all input parameters and their contribution to the uncertainty of model output. In addition, they are capable of taking into account the non-linearity of the model and interactions among input parameters by simultaneously considering the entire distribution of all input parameters [10]. There are two types of GIMs that have been proposed and applied recently: variance-based and moment-independent [8,10]. Variance-based GIMs are simply a modified version of local IMs in order to account for the entire input parameter distribution instead of only the point value [8]. On the other hand, moment-independent IMs consider the probability density function (PDF) or the

cumulative distribution function (CDF) of the model output to estimate the uncertainty importance of model input parameters.

Various authors indicate that local IMs and GIMs may produce different rankings of the input parameters since they evaluate different indices [9,11,13]. For example, E. Borgonovo [14] mentions that local IMs quantify their contribution of input parameters to total risk, while GIMs compute their contribution to the total uncertainty of output. There is, however, a situation where GIMs should be utilized instead of local IMs. If the input parameters are given by their distributions, the GIMs must be performed [14] because the risk model becomes non-linear with the uncertainty of input parameters even if the original expression is linear [11]. This can be seen when considering the simple example of a one-out-of-two parallel system. If the two components are assumed to be independent, the unavailability of the system Q is written as

$$Q = q_1 q_2 \tag{1}$$

where q_1 and q_2 are the unavailability of components 1 and 2, respectively. Equation (1) is linear with respect to each input parameter. Now, we assume both q_1 and q_2 have uncertainty. Then Q becomes a function of random variables. The variance of Q is

$$V[Q] = V[q_1 q_2] = E[q_1^2]\,E[q_2^2] - (E[q_1])^2 (E[q_2])^2 . \tag{2}$$

As seen in equation (2), when uncertainties of input parameters are taken into account, the risk model involves non-linearity.

Because the simulation module in IPRA (Module #2 in Figure 1) has input parameters with distributions and, the output is a complex function of input parameters with non-linearity and interactions among them, the GIM methodology is selected for IPRA. Section 2.2 compares different global approaches and selects one for IPRA.

2.2. Selection of GIM Methodology for IPRA

The GIM methodologies are divided into two categories: variance-based methods [15] and moment-independent methods [8,14]. Both techniques are global and are able to capture the entire distribution of input parameters and interactions among them. However, it has been explained that a variance-based importance measure is insufficient for the purpose of quantifying which input parameters most influence the decision-maker's state of knowledge [8,14,16]. Borgonovo [16] reports that the ranking of input parameters obtained by a variance-based method differs from the one produced by a moment-independent method, especially for the most influential input parameters. In addition, Borgonovo [14] mentions that, when the analyst wants to rank the input parameters based on their impact on the uncertainty of the model output, a sensitivity indicator should refer to the output distribution instead of to its moment, such as variance. Thus, the moment-independent GIM method, which is calculated by referring to output distribution, is selected as an importance measure for our IPRA framework.

In this paper, a moment-independent GIM, called a CDF-based sensitivity indicator $S_i^{(\mathrm{CDF})}$ [8], has been selected for IPRA. This indicator ranks the input parameters based on their influence on the cumulative density function (CDF) of model output calculated by randomly sampling the input parameters. This method is capable of capturing all three key required elements of IM for risk models including (i) distribution of input parameters, (ii) interaction among input parameters in the risk model, and (iii) distribution of the model output.

$S_i^{(\mathrm{CDF})}$ assumes the model output Y as a function of input parameters $X = \{X_1, X_2, \ldots, X_m\}$ expressed by

$$Y = g(X_1, X_2, \cdots, X_n) \tag{3}$$

To begin, input parameters are randomly sampled from their distributions, and with each set of input parameters, the model output Y is calculated. As a result, the unconditional CDF of model output F_Y

(y) can be quantified. Here, the term "unconditional" means that the CDF of model output is calculated by randomly sampling all input parameters from their distributions.

Then, the conditional CDF of model output is calculated using the 'two-loop' Monte Carlo (MC) sampling method [8]. First, one of the input parameters X_i is randomly sampled from its distribution (denoted as x_i^*), which is the first loop of MC sampling. Then, the conditional model output is calculated by fixing the input parameter X_i at x_i^*, while the other input parameters are randomly sampled from their distributions (the second loop of MC sampling). Based on the conditional outputs, the conditional CDF of model output $F_{Y|Xi}(y)$, given that the input parameter X_i is specified at a certain value, is produced. The difference between $F_Y(y)$ and $F_{Y|Xi}(y)$ is measured by the area $A(X_i)$ closed by $F_Y(y)$ and $F_{Y|Xi}(y)$ curves. We can obtain $A(X_i)$ by integrating the absolute difference between $F_Y(y)$ and $F_{Y|Xi}(y)$ along the axis of model output Y.

$$A(X_i) = \int \left| F_{Y|X_i}(y) - F_Y(y) \right| dy \,. \tag{4}$$

These steps are repeated with random samples of x_i^*. Based on the output from replicated calculation of $A(X_i)$, the expected difference of $F_{Y|Xi}(y)$ from $F_Y(y)$ is calculated by

$$E[A(X_i)] = \int f_{X_i}(x_i) A(X_i) dx_i \,, \tag{5}$$

where $f_{xi}(x_i)$ is the marginal density distribution of input parameter X_i.

Q. Liu et al. [8] define the CDF-based sensitivity indicator $S_i^{(\mathrm{CDF})}$ as

$$S_i^{(CDF)} = \frac{E(A(X_i))}{|E(Y)|}, \tag{6}$$

where $E(Y)$ is the unconditional expected value of model output Y.

3. COMPARISION OF GLOBAL METHODS FOR IPRA USING ILLUSTRATIVE EXAMPLES

The IM methodology has not yet been applied to IPRA. This is due to the intrinsic difficulties in applying the traditional/local IM methodologies such as Fussell-Vesely (FV) and Risk Achievement Worth (RAW) [1] to IPRA. Morton et al. [17] proposed a one-way SA procedure for IPRA as an alternative to traditional/local IM methodologies, and presented the preliminary results of its application to the risk-informed resolution of GSI-191. One-way SA is global as it partially considers the distribution of input parameters; however, it does not consider the interactions among the input parameters. For the one-way SA, the nominal values and ranges of input parameters were first determined based on expert opinion. The ranges of parameters were given by appropriate distributions. Then, the one-way SA was performed using a tornado diagram in order to rank the input parameters according to their contributions to the model output.

While the one-way SA has made significant clarifications and advancement on ranking of parameters in IPRA, additional research is needed to resolve its limitations when it is applied to a complex model like IPRA. The limitations include: (1) the one-way SA is not comprehensive with respect to consideration of the distribution of input parameters. Since the one-way SA is conducted by varying the input parameters only within the predetermined ranges (i.e., between lower and upper ranges), it is not capable of capturing the entire distribution of input parameters. This limitation becomes important when the input parameters are given by a non-uniform distribution (e.g., log-normal) in which both the probability density and continuous tails need to be accounted for, (2) during the analysis for a certain input parameter, since only that input parameter is varied, and the other input parameters remain fixed at their predetermined nominal values, the one-way SA is not capable of capturing interactions among

input parameters, and (3) because the sensitivity is evaluated by relying solely on the maximum deviation of the model output from the nominal output, the one-way SA is not able to account for the entire distribution of the model output (e.g., shape of model output distribution).

Morton et al. [17] also suggest the *metamodel* (or *response surface model*) approach to advance the SA. This method can account for cross-term effects of several input parameters that are not considered in the one-way SA approach. Nevertheless, some of the limitations mentioned above would still exist. Limitation #2 would be partially solved since the *metamodel* approach tries to derive the regression equation by fitting the model output within the whole range of input parameters. However, as this approach presumes the form of a regression model, we need to be aware of its effects on the results when selecting a specific type of regression model. Besides, limitation #1 would remain if the ranges of input parameters are predetermined by lower and upper bounds, instead of by sampling input parameters from their distribution.

Therefore, in this paper, the CDF-based sensitivity indicator ($S_i^{(CDF)}$) is suggested as an appropriate moment-independent GIM for IPRA since it can capture all three dimensions that have been identified as the key elements of IM: (1) entire distribution of input parameters, (2) interaction among independent input parameters, and (3) entire distribution of model output. In the following sections, the one-way SA using the tornado diagram [17] and the CDF-based sensitivity indicator $S_i^{(CDF)}$ [8] are applied to three illustrative models; (1) a hypothetical system model composed of four components, , (2) a non-linear mathematical model, and (3) a fault tree without common cause failures and (4) a fault tree with common cause failures. Then, the ranking obtained by each method is compared to illustrate the differences between the one-way SA and GIM methods.

3.1. A Hypothetical System with Four Components

The hypothetical system model analyzed in this section is shown in Figure 2. In this system, the components 1 and 2 are in series, while components 3 and 4 are in parallel. The system fails if either component 1 or 2 fails, or if both components 3 and 4 fail. Each component is assumed to have independent random failure times T_1, T_2, T_3, and T_4. It is also assumed that the failed component is not repaired. The Boolean expression of this system is given by

$$T = X_1 + X_2 + X_3 \cdot X_4 \tag{7}$$

The failure time of the system T is evaluated by:

$$T = \min\{T_1, T_2, \max\{T_3, T_4\}\} \tag{8}$$

Figure 2: An example of a system with four components.

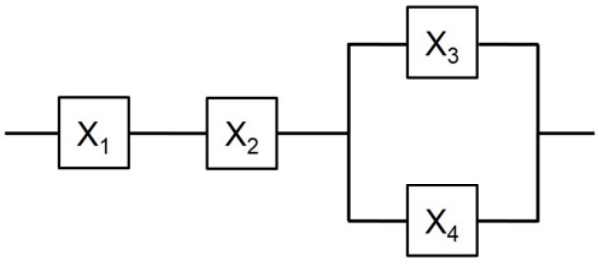

Table 1: Lower and upper bounds of uniform distribution for failure rate.

(Days)	Lower bound	Upper bound
λ_1^{-1}	150	250
λ_2^{-1}	150	250
λ_3^{-1}	25	75
λ_4^{-1}	25	75

In this example, the expected system failure time $E(T)$ is selected as a target model output, where sensitivity to input parameters is analyzed using a one-way SA (tornado diagram) and GIM ($S_i^{(CDF)}$). On the other hand, the input parameters are four independent random variables T_1, T_2, T_3, and T_4. These four input parameters are assumed to obey exponential distribution with a constant failure rate of λ_1, λ_2, λ_3, and λ_4, respectively. The failure rate for each component has an epistemic uncertainty given by a uniform distribution. The lower and upper bounds of uniform distribution are listed in Table 1.

3.1.1. Computational Methods

We followed the method proposed by Clemen et al. [18] for computation of the one-way SA using the tornado diagram. Morton et al. [17] has also used the same method in the SA on an IPRA for the risk-informed resolution of GSI-191. In order to conduct the one-way SA, the nominal values and ranges of input parameters must be identified. The nominal value of each input parameter was set to the mean value of the uniform distribution shown in Table 1. In other words, the nominal value was set to $\lambda_1^{-1} = \lambda_2^{-1} = 200$ [Days] and $\lambda_3^{-1} = \lambda_4^{-1} = 50$ [Days]. On the other hand, the minimum and maximum ranges of each input parameter were set to the lower and upper bounds of uniform distribution.

A tornado diagram (Figure 3) was computed to enable us to compare the relative impact of each input parameter. First, the output $E(T)$ was calculated with one of the input parameters being gradually increased from its minimum to its maximum range, while the other input parameters were fixed at their nominal values. The number of random samplings from the exponential failure curve was set to 3,000. Next, the minimum and maximum values of those outputs were plotted in a horizontal bar chart. In the graph (Figure 3), the nominal output, which means the model output computed by fixing all input parameters at their nominal values, is set as the zero point of the x-axis. The length of each bar illustrates the change of the model output when one of the input parameters is swept from its lower to upper bound. From a tornado diagram, it can be determined which input parameter has the largest impact on the model output.

The $S_i^{(CDF)}$ for a hypothetical system model was computed using the MC simulation-based method proposed by Liu et al. [8]. The unconditional model output Y (in this case, $E(T)$) was calculated by randomly sampling all input parameters from their distribution with a sampling size of n = 10,000. Based on the output, the approximate unconditional CDF of the model output $F_Y(y)$ was calculated by the empirical distribution function $S_Y^n(y)$.

$$S_Y^n = \sum_{j=1}^{n} T(y, y_j) / n \tag{9}$$

$$T(y, y_j) = \begin{cases} 1, & if\ y > y_j \\ 0, & if\ y \le y_j \end{cases} \tag{10}$$

where j denotes the sample index. In other words, the model output y_j was calculated with the randomly sampled set of input parameters $\{x_1^{(j)}, x_2^{(j)}, \ldots, x_n^{(j)}\}$ (j = 1, 2, … ,n). Following the method

explained in Section 2.2, the conditional CDF of model output ($F_{Y|Xi}(y)$) was generated based on equations (9) and (10), as well. Finally, $S_i^{(CDF)}$ of each input parameter was calculated using equations (4) to (6).

3.1.2. Comparison of the Results

Figure 3 shows the tornado diagram for input parameters of the system model in Figure 2. In this graph, the red and blue bars illustrate the change of model output Y when one input parameter is increased or decreased, respectively. In tornado diagrams, the sensitivity of the model output to its input parameters is measured by the length of bars; the longer the bar, the larger the sensitivity of the model.

Table 2 shows the ranking of input parameters based on $Si^{(CDF)}$. In this table, input parameters were ranked based on the mean value of $Si^{(CDF)}$. In addition to the mean value of $Si^{(CDF)}$, Table 2 shows 95% CIs of $Si^{(CDF)}$ for each input parameter. When we rank the input parameters, based on some indices calculated using a sampling methodology, it is important to take into account the CIs that are accompanied with mean values of indices. If the CIs do not overlap each other, then the ranking is statistically significant. Thus, we calculated and presented 95% CIs of $Si^{(CDF)}$ in Table 2, even though the original methods for calculating $Si^{(CDF)}$ proposed by Liu et al. did not include CIs. According to Table 2, $Si^{(CDF)}$ produced the same ranking as a tornado diagram ($\lambda_{3\text{-}1} = \lambda_{4\text{-}1} > \lambda_{1\text{-}1} = \lambda_{2\text{-}1}$). Again, it should be noted that CIs are overlapped between $\lambda_{3\text{-}1}$ and $\lambda_{4\text{-}1,}$ and between $\lambda_{1\text{-}1}$ and $\lambda_{2\text{-}1.}$

Figure 3 shows that the output $E(T)$ is more sensitive to input parameters λ_3^{-1} and λ_4^{-1} compared with λ_1^{-1} and λ_2^{-1}. Since 95 % confidence intervals (CIs) are overlapped between λ_3^{-1} and λ_4^{-1}, there is not enough evidence to conclude the difference in the influence on the output. The same argument arises for input parameters λ_1^{-1} and λ_2^{-1}. Therefore, using the tornado diagram methodology, ranking of the input parameters based on their impacts on the model output was calculated as $\lambda_3^{-1} = \lambda_4^{-1} > \lambda_1^{-1} = \lambda_2^{-1}$.

Table 2 shows the ranking of input parameters based on $S_i^{(CDF)}$. In this table, input parameters were ranked based on the mean value of $S_i^{(CDF)}$. In addition to the mean value of $S_i^{(CDF)}$, Table 2 shows 95% CIs of $S_i^{(CDF)}$ for each input parameter. When we rank the input parameters, based on some indices calculated using a sampling methodology, it is important to take into account the CIs that are accompanied with mean values of indices. If the CIs do not overlap each other, then the ranking is statistically significant. Thus, we calculated and presented 95% CIs of $S_i^{(CDF)}$ in Table 2, even though the original methods for calculating $S_i^{(CDF)}$ proposed by Liu et al. [8] did not include CIs. According to Table 2, $S_i^{(CDF)}$ produced the same ranking as a tornado diagram ($\lambda_3^{-1} = \lambda_4^{-1} > \lambda_1^{-1} = \lambda_2^{-1}$). Again, it should be noted that CIs are overlapped between λ_3^{-1} and λ_4^{-1}, and between λ_1^{-1} and λ_2^{-1}.

Figure 3: Tornado diagram for hypothetical system model

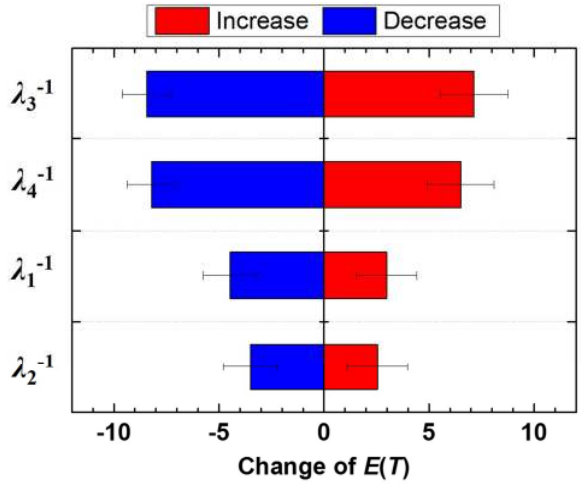

Table 2: Ranking of input parameters in the hypothetical system model based on $S_i^{(CDF)}$

Ranking	Input Parameter	Mean Value $S_i^{(CDF)}$	95 % CI Lower Limit	95 % CI Upper Limit
1	λ_3^{-1}	0.081	0.045	0.118
1	λ_4^{-1}	0.080	0.044	0.117
2	λ_2^{-1}	0.026	0.013	0.039
2	λ_1^{-1}	0.026	0.012	0.039

3.2. A Non-linear Mathematical Model: Ishigami Function

The Ishigami function is a nonlinear and non-monotonic function, which is commonly used to check the performance of SA techniques, e.g., Liu et al. [8] and Borgonovo [14]. The Ishigami function is formulated as

$$Y = \sin X_1 + a \sin^2 X_2 + b X_3^4 \sin X_1 \tag{11}$$

where X_i (i = 1, 2, 3) are three input parameters assumed to be independent from each other. Besides, a and b are parameters and normally set to be 5 and 0.1, respectively. The probability density function for input parameter X_i (i = 1, 2, 3) is given by the uniform distribution in $[-\pi, \pi]$

$$f_{X_i}(x_i) = \begin{cases} 1/2\pi & x_i \in [-\pi, \pi] \\ 0 & x_i \notin [-\pi, \pi] \end{cases} \tag{12}$$

3.2.1. Computational Methods

For the one-way sensitivity analysis (using a tornado diagram), we followed the same method by Clemen et al. [18], as we did in the previous model example. The nominal value was set to 0, corresponding to the mean and median of the distribution given by equation (12). On the other hand, the minimum and maximum ranges of each input parameter were set to $-\pi$ and π, respectively. These correspond to the lower and upper bounds of the uniform distribution for each input parameter, given by equation (12). Then, a tornado diagram was computed to compare the relative impact of each input parameter. The tornado diagram was obtained as follows. First, the output Y of the Ishigami function was calculated with one of the input parameters being gradually increased from its lower to upper bound, while the other input parameters were fixed at their nominal values. Next, the minimum and maximum values of these outputs were plotted on a horizontal bar chart. In the graph, the nominal output, the model output computed with fixing all input parameters at their nominal values, is set as the zero point of the x-axis.

The $S_i^{(CDF)}$ for the Ishigami function was computed using the method explained in Section 3.1.2. For all calculations (unconditional/ conditional model outputs) a sampling size of n = 10,000 was used.

3.2.2. Comparison of the Results

The tornado diagram for input parameters in the Ishigami function is plotted in Figure 4. There is not a bar chart for input parameter X_3 because the sensitivity of model output to the input parameter X_3 is zero when using the tornado diagram method. Viewing Figure 4, we observe that input parameter X_2 appears to be the most sensitive input parameter. The ranking of input parameters, based on its (ranking) impact on model output, was calculated as $X_2 > X_1 > X_3$.

Figure 4: Tornado diagram of input parameters in Ishigami function

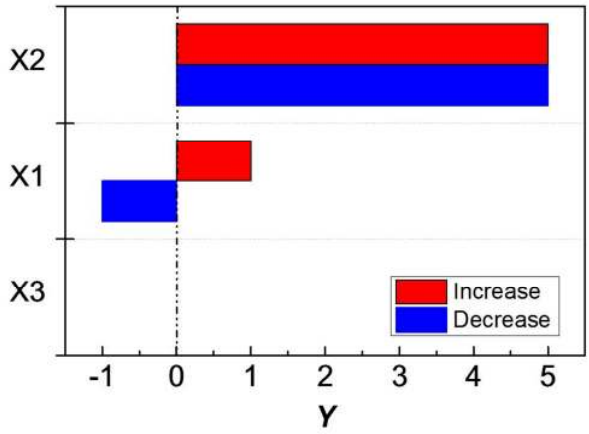

Table 3: Ranking of input parameters in the Ishigami function based on $S_i^{(CDF)}$

Ranking	Input Parameter	Mean Value $S_i^{(CDF)}$	95 % CI Lower Limit	95 % CI Upper Limit
1	X_1	0.834	0.828	0.839
2	X_2	0.686	0.681	0.691
3	X_3	0.450	0.444	0.456

On the other hand, the ranking of input parameters of the Ishigami function obtained by $S_i^{(CDF)}$ is shown in Table 3. This table shows that the ranking of the input parameters are calculated as $X_1 > X_2 > X_3$. As no overlap of 95 % CIs is observed, it can be concluded that this ranking of the input parameters is statistically significant with a 95% confidence level. Both techniques, i.e., using variance-based and moment-independent GIM in references [8,15] reported that X_1 is the most sensitive input parameter. In other words, X_1 has the highest contribution to the variation of the model output. The result of this work is in agreement with the ranking reported by [8] and [15].

In the above calculations, the numbers of samplings were set to n = 10,000 for both layers of MC sampling. Because the $S_i^{(CDF)}$ does not show an overlap among the CIs as presented in Table 3, these numbers of samplings were large enough to get a statistically significant ranking of input parameters. However, when considering the application of $S_i^{(CDF)}$ to a complex simulation model such as the simulation module of GSI-191 project [4], it is desirable to investigate the optimal numbers of random samplings so that we are able to obtain the statistically significant ranking of input variables with as low computational cost as possible. The following demonstrates the preliminary effort of finding the optimized numbers of samplings.

As the first step, we determined the numbers of samplings in the second-layer of MC sampling (denoted as n_2) based on the half-width of 95 % CI of unconditional model output. Namely, the n_2 was selected so that the relative error of the unconditional model output became less than 10 % of the expected value of the unconditional model output. Based on the criteria, we obtained n_2 = 700.

Also, we obtained the numbers of samplings for the first-layer of MC sampling (denoted as n_1) based on the half-width of 95 % CI of $A(X_i)$ as defined in equation (4). First, we computed the standard deviation of $A(X_i)$ (denoted as σ_{20}) with n_2 = 700 (determined previously) and n_1 = 20, which is an arbitrarily chosen value. Then, the optimized value of n_1 was estimated based on the following equation so that the half-width of 95 % CI became less than 10 % of expected value.

Table 4: Ranking of input parameters in the Ishigami function based on $S_i^{(CDF)}$, with the optimized numbers of samplings

Ranking	Input Parameter	Mean Value $S_i^{(CDF)}$	95 % CI Lower Limit	95 % CI Upper Limit
1	X_1	0.802	0.745	0.859
2	X_2	0.632	0.574	0.690
3	X_3	0.407	0.341	0.473

$$\frac{z_{0.025}(\sigma_{20}/\sqrt{n_1})}{E[A(X_i)]} \leq 10\% \qquad (13)$$

where $z_{0.025}$ is z-value corresponding to 5 % significance level, and E [A (X_i)] is the expected value of A (X_i) calculated with n_1 = 20. As a result, the optimized number of n_1 was calculated as n_1 = 90.

Using the optimized value of n_1 = 90 and n_2 = 700, the ranking of input parameters in the Ishigami function was recalculated (Table 4). The ranking of input parameters was calculated as $X_1 > X_2 > X_3$ without overlap of CI. The result demonstrated that the optimized numbers of samplings, which are much less than the original value ($n_1 = n_2$ = 10,000), were large enough to obtain a statistically significant result. This fact indicated the possibility of optimizing the numbers of samplings based on the criteria of relative error in the future application of $S_i^{(CDF)}$ to a complicated and large simulation model (e.g., simulation module in IPRA).

3.3 A Fault Tree Model

As the third example, a tornado diagram and $S_i^{(CDF)}$ were applied to a fault tree model that was first proposed by R. L. Iman [19] in order to check the functionality of the sensitivity analysis method, and was also used by Q. Liu et al. [8]. The Boolean expression of the fault tree model is given by

$$\begin{aligned} Y = {} & X_1X_3X_5 + X_1X_3X_6 + X_1X_4X_5 + X_1X_4X_6 + X_2X_3X_4 \\ & + X_2X_3X_5 + X_2X_4X_5 + X_2X_5X_6 + X_2X_4X_7 + X_2X_6X_7 \end{aligned} \qquad (14)$$

where Y is the occurrence frequency of the top event of the fault tree model. This fault tree model has seven input parameters (X_i, i = 1, 2, ⋯ ,7). Among them, X_1 and X_2 correspond to the initiating events and are given by the number of occurrences per year. On the other hand, the input parameters X_3 through X_7 denote the basic events of the fault tree and are expressed in failure probabilities. In this application, all input parameters are given by a lognormal distribution of mean values and error factors that are summarized in Table 7. All input parameters are assumed to be independent from each other.

3.3.1. Computational Method

As in the two previous examples, we followed the method by Clemen et al. [18] for computation of the one-way SA. The nominal value was set to the median of lognormal distribution for each input parameter. On the other hand, the minimum and maximum ranges of input parameters were set to 5th percentile and 95th percentile of lognormal distribution, respectively. In the graph, the nominal output, the model output computed with fixing all input parameters at their nominal values, is set as the zero point of the horizontal axis.

The $S_i^{(CDF)}$ for the fault tree model was explained in Section 3.1.1.. The sampling size for calculation of conditional/unconditional model output was set to 1,000 in this example.

Table 5: Distribution, mean value, and error factor of the input parameters of fault tree model.

Parameter	Distribution	Mean value	Error factor
X_1	Lognormal	2	2
X_2	Lognormal	3	2
X_3	Lognormal	0.001	2
X_4	Lognormal	0.002	2
X_5	Lognormal	0.004	2
X_6	Lognormal	0.005	2
X_7	Lognormal	0.003	2

3.3.2. Comparison of the Results

The tornado diagram for input parameters of the fault tree model is plotted in Figure 7. This shows that, for both increased and decreased value of each input parameters, the ranking of input parameters based on their one-way influence on the model output (corresponding to the length of bar graph in Figure 7) is calculated as $X_3 > X_1 > X_7 > X_4 > X_5 > X_6 > X_2$.

Besides, the ranking of input parameters in the fault tree model using $S_i^{(CDF)}$ is shown in Table 8 as well as the mean value and 95 % CI of $S_i^{(CDF)}$ for each input parameter. Based on the mean value of $S_i^{(CDF)}$, those input parameters are ranked as $X_3 > X_1 > X_7 > X_4 > X_5 > X_6 > X_2$, the same ranking as Q. Liu et al. [8]. This ranking is in agreement with the result from the tornado diagram (Figure 7). Meanwhile, because there is no overlap between 95 % CIs, this ranking based on $S_i^{(CDF)}$ is statistically significant.

Figure 5: Tornado diagram of input parameters for the fault tree model.

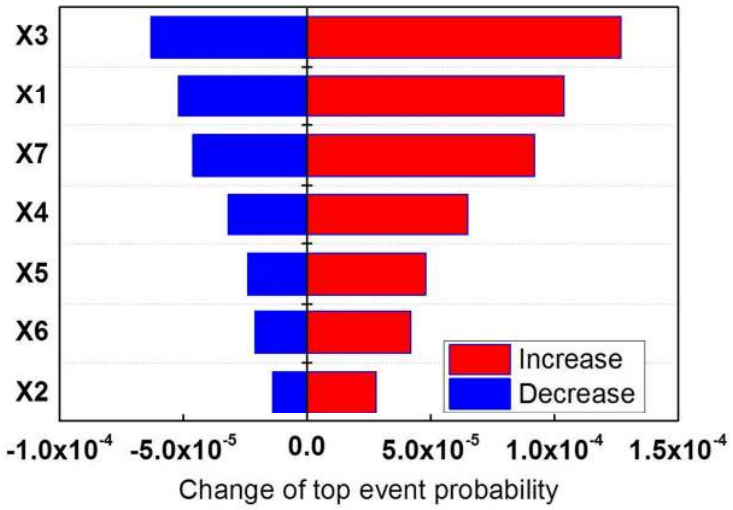

Table 6: Ranking of input parameters in the fault tree model based on $S_i^{(CDF)}$

Ranking	Input Parameter	Mean Value $S_i^{(CDF)}$	95 % CI Lower Limit	95 % CI Upper Limit
1	X_2	0.273	0.261	0.284
2	X_6	0.223	0.214	0.233
3	X_5	0.200	0.192	0.209
4	X_4	0.146	0.139	0.152
5	X_7	0.115	0.110	0.119
6	X_1	0.102	0.098	0.106
7	X_3	0.076	0.073	0.078

3.4 A Fault Tree Model : Involving Common Cause Failure

A tornado diagram and $S_i^{(CDF)}$ are applied to a fault tree model of a hypothetical system involving common cause failure (CCF). The block diagram of the hypothetical system is illustrated in Figure 6. In this system, the D components are identical redundant components that are subjected to CCF. The Boolean expression of the fault tree model is given by

$$T = A + B \cdot C + D_{1,I} \cdot D_{2,I} \cdot D_{3,I} + D_{123,C} \tag{15}$$

where T is the top event of the fault tree model. In this equation, $D_{j,I}$ (j = 1, 2, 3) denotes the probability of independent failure of D components, while $D_{123,C}$ denotes the CCF of redundant D components. Here, the CCF of redundant components is modeled by the beta factor approach. The probability of the top event (T) is formulated by

$$\Pr(T) = \Pr(A) + \Pr(B) \cdot \Pr(C) + \left[(1-\beta) \cdot \Pr(D_T)\right]^3 + \beta \cdot \Pr(D_T) \tag{16}$$

where Pr (D_T) is the probability of failure of component D in total (i.e., the sum of independent and CCF of component D), and β is the beta factor for redundant D components that is defined as the ratio of CCF to the total failure.

All the input parameters of the fault tree model (i.e., failure probabilities of components and beta factor) are given by distribution, as listed in Table 7. The failure probabilities of components are given by lognormal distribution, of which mean value and error factor are shown in Table 7. Besides, the beta factor for the CCF of redundant component D is given by a uniform distribution, of which lower and upper bounds are shown in Table 7. During the computation of top event probability in equation (16), all input parameters are assumed to be independent from each other.

Figure 6: Block diagram of the hypothetical fault tree model

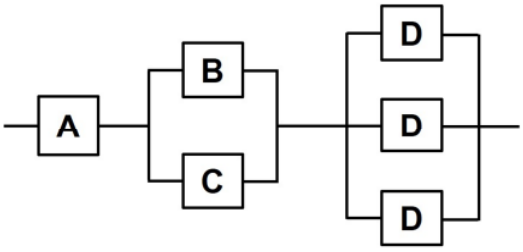

Table 7: Distribution for the input parameters of fault tree model

Parameter	Distribution	Mean value	Error factor
A	Lognormal	2.0×10^{-5}	2.0
B	Lognormal	7.0×10^{-4}	4.0
C	Lognormal	3.0×10^{-4}	4.0
D_T	Lognormal	1.0×10^{-3}	1.6

Parameter	Distribution	Lower bound	Upper bound
β	Uniform	0.05	0.15

3.4.1. Computational Method

Similar to the previous two examples, we followed the method by Clemen et al. [18] for computation of the one-way SA using the tornado diagram. The nominal value was set to the median of distribution for each input parameter. On the other hand, the minimum and maximum ranges of input parameters were set to the 5th percentile and the 95th percentile of distributions, respectively. Then, the tornado diagram was obtained as follows. First, the probability of top event (T) of the fault tree model given by equation (16) was calculated with one of the input parameters being gradually increased from its minimum to maximum ranges, while the other input parameters were fixed at their nominal values. Next, the minimum and maximum values of these outputs were plotted on a horizontal bar chart. In the graph, the nominal output, the model output computed with fixing all input parameters at their nominal values, is set as the zero point of the horizontal axis.

The $S_i^{(\mathrm{CDF})}$ for the fault tree model was explained in Section 3.1.1. The sampling size for calculation of conditional/unconditional model output was set to 2,000 in this example.

3.4.2. Comparison of the Results

The tornado diagram for input parameters of the fault tree model is plotted in Figure 7. Based on the length of the bar graph, the total failure probability of component D (D_T) has the largest influence on the model output (i.e., the probability of top event), followed by beta factor (β) and the failure probability of component A. According to Figure 7, the failure probabilities of components A and B contribute little to the change of top event probability. This indicates that both components A and B are not significant in terms of the influence on the model output. Therefore, the ranking of input parameters based on their one-way influence on the model output is obtained as $D_T > \beta > A >> B \sim C$.

Meanwhile, the ranking of input parameters in the fault tree model using $S_i^{(\mathrm{CDF})}$ is shown in Table 8. Based on the mean value of $S_i^{(\mathrm{CDF})}$, the beta factor (β) is ranked the first, followed by the total failure probability of component D (D_T) and failure probability of component A. Besides, the mean values of $S_i^{(\mathrm{CDF})}$ for the failure probability of components B and C are relatively small compared with those for other input parameters, and we are not able to rank them separately since their 95 % CIs overlap with each other. As a result, $S_i^{(\mathrm{CDF})}$ produces the ranking of input parameters as $\beta > D_T > A >> B \sim C$. This is not in agreement with the result of the one-way SA method in the ranking for first and second most significant input parameters.

Figure 7: Tornado diagram of input parameters for the fault tree model

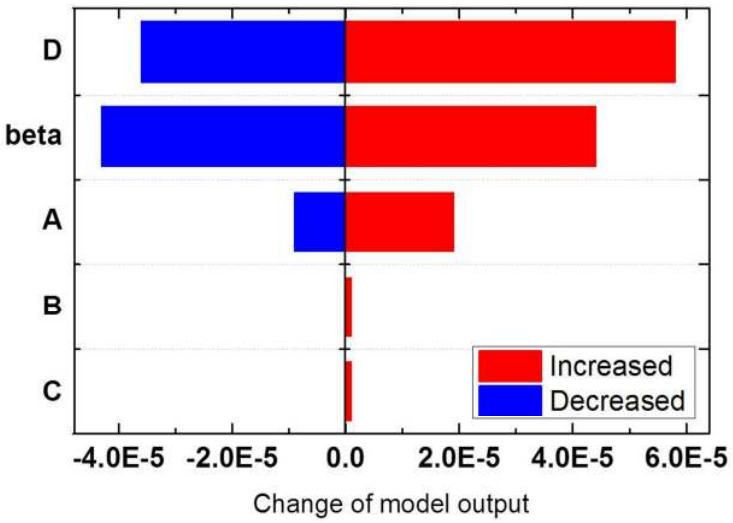

Table 8: Ranking of input parameters in the fault tree model based on $S_i^{(CDF)}$

Ranking	Input Parameter	Mean Value $S_i^{(CDF)}$	95 % CI Lower Limit	95 % CI Upper Limit
1	β	0.2241	0.2196	0.2286
2	D_T	0.2091	0.2031	0.2151
3	A	0.0574	0.0552	0.0596
4	B	0.0137	0.0135	0.0139
4	C	0.0135	0.0133	0.0137

3.5. Discussion

According to the results in previous sections, the one-way SA using a tornado diagram produced the same ranking as GIM ($S_i^{(CDF)}$) for the hypothetical system model (Section 3.1) and for the first fault tree model (section 3.3), but it produced a different ranking for the Ishigami function (Section 3.2) and the second fault tree model involving CCF (Section 3.4). This difference indicates that the one-way SA possibly leads to a different ranking from GIM when the risk model is defined by a non-linear function. Here, non-linearity means that a risk model involves the correlation among the input parameters. In other words, if the first derivative of risk model with respect to every input parameter is constant, then the risk model is linear. When the first derivative is not constant, the risk model is considered as non-linear. In that sense, the Ishigami function is clearly non-linear since the first partial derivative of the function (Equation (11)), with respect to an input parameter always results in the function of that input parameter. The second FT model (Section 3.4) is also non-linear. On the other hand, the four-component hypothetical system model (Section 3.1) and the first FT model (Section 3.3) are linear since the first partial derivative of risk function is a constant with respect to input parameters. In a complex computational model, such as the simulation module in IPRA, the risk model, in most cases, involves a non-linearity since the input parameters can naturally have the correlation among each other that is induced by the common underlying physical mechanics.

The difference in rankings by the one-way SA and GIM on a non-linear model has several causes. First, a tornado diagram ranks input parameters based on the maximum deviation of model output value from its nominal output value (i.e., the output computed with setting all input parameters to their

nominal values). However, $S_i^{(CDF)}$ ranks input parameters based on the change of the entire CDF of the model output. When we evaluate the impact of uncertainty of input parameters on the uncertainty of model output, it is necessary to account for the entire distribution of the model output [8]. Thus, the ranking of the $S_i^{(CDF)}$ method is considered to be more informative and accurate than the ranking based on a tornado diagram. Second, the difference is related to the manner of varying the input parameters during the analysis. In a tornado diagram, only one input parameter is varied from its lower to upper bound, while the other input parameters are fixed at their nominal values. This is why a tornado diagram is categorized as "one-way sensitivity analysis". On the other hand, $S_i^{(CDF)}$ is computed by randomly sampling all input parameters from their distributions. When we rank the input parameters given by distributions, the "global" analysis is needed to take into account the entire distribution of input parameters and the interactions among them. Therefore, the ranking by $S_i^{(CDF)}$ reflects more information on the ranking than that of a one-way SA method such as a tornado diagram.

Moreover, a tornado diagram presents a difficulty in choosing appropriate nominal values for input parameters. In Figure 4, the sensitivity of the model output to input parameter X_3 was computed to be zero. This result is questionable when compared to the ranking based on $S_i^{(CDF)}$. The zero sensitivity to input parameter X_3 is caused by the selection of nominal values of the other input parameters ($X_1 = 0$ and $X_2 = 0$) rather than the nature of the model output. This example illuminates the potential difficulty in choosing nominal values and ranges of each input parameter, and this is one of the main motivators for considering the adoption of the GIM for the application to the IPRA.

4. CONCLUSION

In this paper, an IM methodology suitable for an *integrated* PRA (IPRA) framework for Nuclear Power Plants (NPPs) is investigated. In IPRA, the classical PRA of the plant is used, but specific areas of concern (e.g., fire, GSI-191, organizational factors, and seismic) are modeled in a simulation-based module (separate from PRA) and the module is then linked to the classical PRA of the plant. Because of the complexity and non-linearity of IPRA, the conventional/local IMs (e.g., FV, RAW) may be less informative for such IPRA, and, so this research compares the local and Global Importance Measure (GIM) methodologies and explains the importance of GIM for IPRA.

The research also demonstrates the application of two types of global methodologies (i.e., the one-way SA and the CDF-based $S_i^{(CDF)}$, as a moment-independent GIM) to four illustrative example models (i.e., a hypothetical system model, a non-linear mathematical model, and two fault tree models) and, based on the comparison of the results, selects the CDF-based $S_i^{(CDF)}$ as an appropriate IM for IPRA. The results conclude that for a non-linear risk model, the two methods produce a different ranking of input parameters. In addition, they indicate that when the one-way SA is applied to a complex risk model, the analyst may have difficulty in selecting the appropriate nominal values for the input parameters. The CDF-based $S_i^{(CDF)}$ is more accurate than the local IM and one-way SA because it can capture three key features: (1) distribution of input parameters, (2) interactions among input parameters, and (3) distribution of the model output. When applying CDF-based $S_i^{(CDF)}$, the analyst should consider careful selection of sampling approach. As shown in the result on Ishigami function, the number of random sampling determines the width of confidence interval, and thus, it has a crucial effect on the decision-making involving the identification of risk-significant factors based on the ranking of input parameters. The result of investigation on the optimized number of random sampling (Section 3.2.3) indicates that the criteria based on relative error can be used to estimate the optimal number of sampling. As a work in progress, the CDF-based $S_i^{(CDF)}$ method is being applied to IPRA in the risk-informed resolution of GSI-191 [4]. A future paper will report on the results of this GSI-191 GIM study.

References

[1] M. Van der Borst and H. Schoonakker, "An overview of PSA importance measures," *Reliability Engineering and System Safety*, no. 72, pp. 241-245, 2001.

[2] Z. Mohaghegh, A. Mosleh and R. Kazemi, "Incorporating Organizational Factors into Probabilistic Risk Assessment (PRA) of Complex Socio-technical Systems: A Hybrid Technique Formalization," *Reliability Engineering and System Safety*, vol. 94, issue 5, pp. 1000-1018, 2009.

[3] J. Pence, Z. Mohaghegh, C. Ostroff, E. Kee, F. Yilmaz, D. Johnson and R. Grantom, "Toward an Internet of Organizational Safety Indicators by Integrating Probabilistic Risk Assessment, Socio-Technical Systems Theory, and Big Data Analytics", in *Proceedings of 12th International Topical Meeting on Probabilistic Safety Assessment and Analysis (PSAM12)*, 2014.

[4] Z. Mohaghegh, E. Kee, S. Reihani, R. Kazemi, D. Johnson, R. Grantom, K. Fleming, T. Sande, B. Letellier, G. Zigler, D. Morton, J. Tejada, K. Howe, J. Leavitt, H. Yassin, R. Vaghetto and S. ??and Lee, "Risk-Informed Resolution of Generic Safety Issue 191," In *Proceedings for International Topical Meeting on Probabilistic Safety Assessment and Analysis (PSA2013)*, 2013.

[5] T. Sakurahara, Z. Mohaghegh, E. Kee, S. Reihani, R. Kazemi and M. Brandyberry, "A New Integrated Framework to Advance Fire Probabilistic Risk Analysis of Nuclear Power Plants," In *Proceedings of 2013 American Nuclear Society, Risk Management Topical Meeting*, 2013.

[6] T. Sakurahara, S. Reihani, Z. Mohaghegh, M. Brandyberry, E. Kee, F. Yilmaz, S. Rodgers, M. Billings and D. Johnson, "Developing A New Fire PRA Framework by Integrating Probabilistic Risk Assessment with Fire Simulation Module," in *Proceedings for 12th International Topical Meeting on Probabilistic Safety Assessment and Analysis (PSAM12)*, 2014.

[7] A. Elbanna, Z. Mohaghegh, E. Kee, S. Reihani, R. Kazemi and S. Rodgers, "Toward a Physics-based Seismic PRA," In *Proceedings of 2013 American Nuclear Society, Risk Management Topical Meeting*, 2013.

[8] Q. Liu and T. Homma, "A New Importance Measure for Sensitivity Analysis," *Nuclear Science and Technology*, vol. 47, pp. 53-61, 2010.

[9] H. M. Wainwright, S. Finsterle, Y. Jung, Q. Zhou and J. T. Birkholzer, "Making sense of global sensitivity analyses," *Computers & Geosciences*, vol. 65, pp. 84-94, 2013.

[10] T. Aven and T. E. & Nøkland, "On the use of uncertainty importance measures in reliability and risk analysis," *Reliability Engineering & System Safety*, vol. 95, no. 2, pp. 127-133, 2010.

[11] E. Borgonovo, G. Apostolakis, S. Tarantola and A. Saltelli, "Comparison of global analysis techniques and importance measures in PSA," *Reliability Engineering and System Safety*, vol. 79, pp. 175-185, 2003.

[12] A. Saltelli, M. Ratto, T. Andres, F. Campolongo, J. Cariboni, D. Gatelli , and S. Tarantola, "Global sensitivity analysis: the primer," John Wiley & Sons, 2008.

[13] R. Tebbens, M. Pallansch, O. Kew, R. Sutter, R. Aylward, M. Watkins, H. Gary, J. Alexander, H. Jafari, S. Cochi and K. Thompson, "Uncertainty and Sensitivity Analyses of a Decision Analytic Model for Posteradication Polio Risk Management," *Risk Analysis*, vol. 28, no. 4, pp. 855-876, 2008.

[14] E. Borgonovo, "A new importance measure," *Reliability Engineering and System Safety*, vol. 92, pp. 771-784, 2007.

[15] I. Sobol, "Global sensitivity indices for nonlinear mathematical models and their Monte Carlo estimates," *Mathematics and Computers in Simulation*, vol. 55, pp. 271-280, 2001.

[16] E. Borgonovo, "Measuring Uncertainty Importance: Investigation and Comparison of Alternative Approaches," *Risk Analysis*, vol. 26, no. 5, pp. 1349-1361, 2006.

[17] D. Morton, B. Letellier, J. Tejada, D. Johnson, Z. Mohaghegh, E. Kee, V. Moiseytseva, S. Reihani and A. Zolan, "Sensitivity Analyses for a High-Order Simulation Used in the STP GSI-191 Risk-Informed Resolution Project," In *Proceedings of 2014 22nd International Conference on Nuclear Engineering (ICONE22)*.

[18] R. Clemen and T. Reilly, "Making Hard Decision with Decision Tools (3rd edition)," Mason, OH: South-Western, 2001.

[19] R. L. Iman, "A matrix-based approach to uncertainty and sensitivity analysis for fault tree," *Risk Analysis*, vol. 7, no. 1, pp. 21-33, 1987.